Computation of Temperature Elevation in a Foetus Exposed to Ambient Heat and Radio Frequency Fields

Akimasa Hirata, Ilkka Laakso, Yuri Ishii, Tomoki Nomura, and Kwok Hung Chan

Department of Computer Science and Engineering, Nagoya Institute of Technology, Nagoya 466-8555, Japan

Corresponding Author: Akimasa Hirata

E-mail: ahirata@nitech.ac.jp

abstract

Temperature elevation in the foetus is of concern for excess heat load including that from radio-frequency exposure. No previous study succeeded in simulating the temperature difference between the mother and foetus. This study develops a thermal model for a pregnant woman and then applies it to simulate the temperature variations due to ambient heat exposure and RF exposure. When the pregnant woman model is exposed to ambient temperature of 35–45 °C, the core temperature elevations in the mother and the foetus are almost identical. Contrarily, the foetal temperature elevation for radio-frequency exposure is higher than that in the mother.

Keywords: bioheat equation, core temperature, electromagnetic wave exposure, environmental heat exposure, thermal modelling of biological system

NOMENCLATURE

A	basal metabolism	V	total volume
B	blood perfusion rate	ρ	mass density
C	specific heat		
F	weighting coefficients	Subscripts	
H	heat transfer coefficient	$(\,)_{bf}$	associated with the foetus
K	thermal conductivity	$(\,)_{bm}$	associated with the mother
Q_b	heat exchange	$(\,)_B$	associated with the blood
	between the blood and tissue	$(\,)_e$	associated with the air
Q_{BT}	rate of heat acquisition	$(\,)_{HB}$	signal from the hypothalamus
S	surface area	$(\,)_s$	associated with the skin
T	temperature of the tissue	$(\,)_{SB}$	signal from the skin

1. INTRODUCTION

Numerical modeling of heat transfer in biological tissue has been extensively conducted in different application [1-7]. Temperature variation in the foetus is of interest to estimate for excess heat load. For example, other limits were suggested for pregnant women in the hot tub and sauna considering adverse effects in foetus [8]. However, the time course of temperature elevation in the foetus has not been reported for excess heat stress, in part due to ethical reason. In addition, there has been increasing public concern regarding the adverse health effects of exposure to a radio frequency (RF) field. The thermal effect in the human body is one of the dominant effects of field exposure. As listed in the high priority research by the World Health Organization [9], the temperature elevation in the foetus due to RF exposure should be evaluated.

Thermal modeling of foetus has been conducted mainly to investigate the temperature elevation for RF exposure in magnetic resonance (MR) systems. The limit of the temperature elevation during MR exposure should be set as less than 0.5 ℃ according to the international standard for 'normal mode' operation, corresponding to no physiological stress to patients [10]. Temperature elevation in the foetus due to exposure from MR equipment was computed assuming that the blood temperature elevation in the mother and foetus were constant at 37 ℃ and neglecting the thermophysiological response [11]. In [12], the blood temperature in the mother and foetus were constant at 37 and 37.5 ℃, respectively; the thermophysiological response was also not considered. However, both the blood temperature elevation and the thermoregulatory response cannot be neglected for power absorption, characterized by whole-body averaged specific absorption rate [13] larger than 0.4 W/kg [14]. Kikuchi, et al. [15] calculated the foetus temperature by considering the blood temperature variation using a method proposed in [16]; the blood temperature variation is assumed to be uniform throughout the body but varies with time to satisfy the thermodynamics law. However, Kikuchi, et al. [15] did not consider that the blood circulating in the foetus and its mother is different [17]; thus, the variation of blood temperature should be different in the foetus and mother. Note that the temperature in the foetus has been reported to be 0.3−0.5 ℃ higher than that in the mother in the thermoneutral condition[17, 18]. Owing to the above-mentioned assumptions, the temperature difference between the foetus and its mother could not be simulated computationally in previous studies [12, 15].

The purpose of the present study is to develop a new thermal model for a pregnant woman in which the thermal exchange between the mother and the foetus in the placenta is taken into account. Then, the foetal and maternal temperature elevation for ambient temperature and RF exposure is investigated.

2. MODEL AND METHODS

2.1. Human body model

The numeric Japanese pregnant woman model was developed based on the adult female model named HANAKO [19] which is segmented into 51 tissue types/organs such as skin, muscle, bone, brain, heart, etc. The pregnant woman model at a gestation of 28 weeks has 56 tissue

types/organs including the foetal brain and eyes and the placenta [20]. The height and the weight of the model are 1.59 m, and 59 kg, respectively. The resolution of the human model is 2 mm. Note that the umbilical vessels are not considered in the pregnant woman model unlike in previous study [12]. However, this assumption affects computational results marginally because the heat exchange mainly occurs in the placenta.

2.2. Method for thermal dosimetry

The computational algorithm for thermal dosimetry is given in our previous study [16]. The bioheat equation are coupled with the equation governing the thermoregulatory response, and discretised in time domain. In the present study, the algorithm is further developed to include the heat exchange between the mother and foetus. The method is reviewed briefly.

Temperature variation in the numeric human model was calculated by solving a bioheat equation [21], which is an equation for modelling thermodynamics in the human body:

$$C(\vec{r})\cdot\rho(\vec{r})\frac{\partial T(\vec{r},t)}{\partial t}=\nabla\left(K(\vec{r})\cdot\nabla T\right)+SAR(\vec{r},t)+A(\vec{r},t)-Q_b(\vec{r},t) \tag{1}$$

where $T(\vec{r},t)$ is the temperature of the tissue, C is the specific heat of the tissue, ρ is the mass density of the tissue, K is the thermal conductivity of the tissue, A is the basal metabolism per unit volume, and Q_b heat exchange between the blood and tissue per unit volume.

In the present study, the heat exchange in the placenta was considered so that the maternal and foetal blood circulate in the placenta. To simulate the maternal placental and foetoplacental circulation from the standpoint of thermophysiology, we propose the following equations to represent the term Q_b in (1):

$$Q_b(\vec{r},t)=\begin{cases} B_m(\vec{r},t)\cdot\left(T(\vec{r},t)-T_{bm}(t)\right) & \text{,mother} \\ B_m(\vec{r},t)\cdot\left(T(\vec{r},t)-T_{bm}(t)\right)+B_f(\vec{r},t)\cdot\left(T(\vec{r},t)-T_{bf}(t)\right) & \text{,placenta} \\ B_f(\vec{r},t)\cdot\left(T(\vec{r},t)-T_{bf}(t)\right) & \text{,fetus} \end{cases} \tag{2}$$

where T_{bm} and T_{bf} are the blood temperatures of the mother and foetus, respectively, and B is a blood perfusion rate and tissue specific parameter. Therefore, there are two mechanisms of heat exchange between the mother and foetus: one is the conduction of heat through the amniotic fluid, and the other is the exchange of heat between the maternal and foetal blood at the placenta. From the original blood perfusion rate of the placenta, the volume ratio of the maternal to foetal blood is divided into 2:1[17].

One of the features in our computational method is that the core temperature variation can be tracked in addition to that in the shallow regions of the body. The blood temperatures of the mother and foetus are considered separately, and they vary according to the following equation, in order to satisfy the first law of thermodynamics [22]:

$$T_{B,n}(t) = T_{B0,n} + \int_t \frac{Q_{BT,n}(t)}{C_B \rho_B V_{B,n}} \mathrm{d}t \tag{3}$$

where T_B is the blood temperature of the mother or foetus, and T_{B0} is its initial blood temperature. Note that the blood temperature is assumed to be constant as one variable over the body in the thermal computational methods including the bioheat equation. Q_{BT} is the net rate of heat acquisition by the blood from body tissues, C_B (= 4,000 J/kg·°C) is the specific heat of blood, and ρ_B (= 1,050 kg/m^3) is the mass density. The subscript n (n = 1,2) represents the foetus and the mother, respectively. V_B is the total volume of blood, which was chosen to be 5,000 ml for the mother and 70 ml for the foetus [23].

The boundary condition between air and tissue in (1) is expressed as:

$$-K(\vec{r})\frac{\partial T(\vec{r},t)}{\partial t} = H(\vec{r}) \cdot \left(T_s(\vec{r},t) - T_e(t)\right) + 40.6 \cdot \left(SW\left(\vec{r}, T_s(\vec{r},t)\right) + PI\right) / S \tag{4}$$

where H, T_s, and T_e denote the heat transfer coefficient, the body surface temperature, and the air temperature, respectively. The heat transfer coefficient, which is given in the formula by Fiala, et al. [24], includes the convective and radiative heat losses. S is the surface area of the human body, SW [g/min] is the sweating rate, and PI (= 0.63 g/min) is the insensible water loss from the skin and the respiratory tract. The value of 40.6 is a conversion coefficient [J min/ g/s]. The sweating rate is modelled based on the formula proposed by Fiala, et al. [25], which is governed by the average skin and core temperature elevations. A detailed description and validation for the sweating model can be found in our previous study [16, 26], which are mostly taken from Duck [27].

Maternal thermal parameters (specific heat, the thermal conductivity and the basal metabolism per unit volume) are identical to those used in our previous study [16]. Note that these parameters are considered as organ/tissue specific values. However, different basal metabolic rates are given between the foetal and maternal tissue. Specifically, the thermal parameters for the foetal tissue are taken from Groen and Bosch [12]. It should be note that the thermal constants in the mother with and without the pregnancy are marginally different except for the increase of the basal metabolism caused by the foetus. For the set of thermal parameters, the basal metabolic rates in the mother and foetus are 1.4 W/kg and 3.8 W/kg, respectively, which are in good agreement with the measured/estimated values of 1.2 W/kg and 3.5−4.5 W/kg [28].

For temperature elevation above a certain level, the blood perfusion rate is increased in order to carry away the excess heat produced. The variation of the blood perfusion rate in the skin through vasodilatation is expressed in terms of ΔT_H and ΔT_S:

$$B(\vec{r},t) = \left(B_0(\vec{r}) + F_{HB}\Delta T_H(t) + F_{SB}\Delta T_S(t)\right) \cdot 2^{(T(\vec{r},t)-T_0(\vec{r}))/6} \tag{5}$$

where F_{HB} and F_{SB} are the weighting coefficients of signal from the hypothalamus and skin, respectively. The coefficients F_{HB} and F_{SB} in Eq. (5) are 17,500 $W/m^3/^oC^2$ and 110 $W/m^3/^oC^2$ [29]. Note that the blood perfusion rate in the skin is assumed to be constant in the foetus, corresponding to no thermoregulatory response. The blood perfusion in all tissues except the skin was considered as constant, which is similar to [30].

The effectiveness of this computational algorithm was verified by comparing the measured and computed temperatures of the skin and body core in the adult female without pregnancy when changing the ambient temperature [26].

2.3. Method for electromagnetic dosimetry

The finite-difference time-domain (FDTD) method was used for calculating the power absorption in an anatomically based human model. An in-house FDTD code, which was validated via inter-comparison, was used [31]. To incorporate the anatomically based model into the FDTD method, the frequency-dependent electrical constants of the tissues are required. These values were taken from a formula based on measurements by Gabriel, et al. [32]. The computational region was truncated by applying a twelve-layered perfectly matched layer absorbing boundary.

2.4. Exposure scenario

Two exposure scenarios were considered: ambient heat exposure and RF exposure. For both scenarios, the pregnant woman model with nude condition was assumed to be standing in free space. For ambient heat exposure, the ambient temperature was changed from 28 °C, which is the thermoneutral condition, to 35, 40, and 45 °C at time $t = 0$.

For RF exposure, a plane wave with a vertical polarization was considered. Note that plane wave exposure is considered instead of exposure from actual MR systems, because international guidelines consider this scenario. The ambient temperature was set as 28 °C. The plane wave was incident on the body model from the front (along the anteroposterior direction). The frequencies of the electromagnetic waves were chosen as 45, 80, and 500 MHz. At 80 MHz, the whole-body averaged SAR became maximal due to the standing wave along the body height direction for exposure in free space [33]. The duration of exposure was chosen as 1 hour. This duration was chosen so as to be longer than the averaging time of 30 min considered in the ICNIRP guidelines [34] and the thermal time constant for a male with a lower perspiration rate (40–50 min) in our previous study [16]. The relative humidity of 50% and wind speed of less than 0.1 m/s was assumed through the computation.

3. COMPUTATIONAL RESULTS

For the thermoneutral condition at an ambient temperature of 28 °C, the thermal balance of the adult female model without pregnancy was maintained [26]; blood temperature did not change from 37.0 °C. Then, the temperature in the pregnant woman model was calculated for the same

parameters to reach a thermally steady state, as shown in Fig. 1. The maternal and foetal blood temperatures were 37.16 and 37.41 °C, respectively. The higher blood temperature in the foetus is attributable to the higher basal metabolic rate of the foetus [17]. The temperature in the hypothalamus (as a surrogate of core temperature) in the foetus and mother were 37.16 and 37.49 °C, respectively. This temperature difference of 0.33 °C is in good agreement with measured data of 0.3−0.5 °C[18].

For heat exposure at 3 ambient temperatures of 35, 40, and 45 °C, the blood temperature elevations in the foetus and its mother were tracked and are shown in Fig. 2. The same tendency was observed in the blood temperature elevation between the foetus and its mother. The blood temperature difference was 0.25 °C at the initial condition. This difference did not change significantly (0.25−0.28 °C) during the exposure even for different ambient temperatures.

For plane-wave exposure of the whole-body averaged SAR of 2 W/kg and 4 W/kg at 80 MHz, the temperature variation and relative difference of maternal and foetal blood are shown in Fig. 3. The maternal and foetal temperatures were 37.56 and 37.91 °C, respectively. This difference of 0.35 °C was larger than that at the initial state of 0.25 °C.

In order to confirm this tendency further, the temperature elevation of maternal and foetal blood and their difference were investigated in figures 4 (a) and (b) for different whole-body averaged SARs and frequencies. Note that the averaged SARs for the foetus were 0.97 W/kg at 46 MHz, 2.65 W/kg at 80 MHz and 1.03 W/kg at 500 MHz when the whole-body averaged SAR in the pregnant woman model was 4.0 W/kg. As shown in figure (a), core temperature elevation becomes large with the increase of whole-body averaged SAR. Marginal nonlinearlity may be attributable to the sweating, as discussed in Hirata, et al. [23] of the From figure 4 (b), the temperature difference increased with the increase of whole-body averaged SAR, and was frequency dependent. The electromagnetic energy absorbed by the foetus may have contributed to the blood temperature elevation of the foetus. Note that the heat generated in the biological tissue diffuses by a few centimetres, and thus the energy absorbed around the foetus also contributed to the foetal blood temperature [35].

4. DISCUSSION

In previous studies, the blood temperature in the foetus and its mother were either considered separately but assumed not to vary with time [12] or assumed to be constant over the foetus and its mother but to vary with time [15]. In the present study, the body temperatures in the foetus and its mother were represented systematically by introducing Eqs. (2) and (3), and the computed data are in good agreement with the measured data at the thermally steady state without any heat load. Further validation is difficult because measured data of foetus for environmental heat exposure is not available as far as the authors know, in particular for the unique core temperature elevation in the foetus for RF exposure, as shown in figure 4.

One of the weaknesses of our modeling is that the umbilical vessels are not considered in the pregnant woman model used here, and thus its impact on the modeling cannot be evaluated.

However, the maternal and foetal blood temperature is assumed to be uniform over the body but variable as time. Thus the heat exchange between the umbilical vessels does not affect the fetal blood temperatures significantly.

For ambient heat exposure where the heat load exists on the body surface only, the blood temperature elevations in the foetus and its mother were almost identical for different ambient temperatures ranging from 35 ºC to 45 ºC. For RF exposure, the blood temperature elevations in the foetus and its mother were different, particularly when the whole-body averaged SAR was high. The temperature difference between the mother and foetus was increased to 0.36 ºC, which is larger than the original value of 0.25ºC. This phenomenon cannot be represented by the models in the previous studies [12, 15]. This different tendency between the ambient heat exposure and RF exposure was attributable to the electromagnetic power absorbed in/around the foetus.

The difference between maternal and foetal blood temperature of 0.25-0.36 ºC is approximate difference from Kikuchi, et al. [15], in which foetus temperature would be underestimated. In addition, core temperature elevation in figure 4 (a) corresponds to the difference between our modeling and that in [21]. From figure 4 (b) , the model used by Hand et al. [12] appears to be reasonable for whole-body averaged SAR of 0.4 W/kg or less because the blood temperature difference does not change. Note that the actual temperature difference between the foetus and its mother reported here would be smaller because the duration considered herein was 60 min, while the duration for MR equipment is less than 20 min [7].

Let us discuss some computational uncertainty and variability of temperature elevation which is attributable to thermal parameters. According to our previous studies [14, 16], the dominant factor affecting core temperature elevation is the sweating rate. The individual difference of sweating may affect the core temperature elevation by 30% or so. In addition, the sweating is governed by the average skin and core temperatures. Recently, new thermal was proposed around the body surface [36]. The use of this thermal model may result in some difference of skin temperature for larger whole-body averaged SAR, leading to some alternation of sweating. On the contrary, in that study, the core temperature elevation was not evaluated, and thus difficult to discuss the modeling effect quantitatively. However, that modeling may not affect the maternal and foetal core temperature *difference* significantly, because the foetal temperature is mainly characterized by the basal metabolic rate and the blood perfusion rate in the placenta.

5. SUMMARY

In the present study, a new thermal model for the pregnant woman model was proposed, and it is an extension of our thermal model which can take into account the blood temperature variation. This thermal model was applied to simulate the temperature variations in the pregnant woman due to ambient heat exposure and RF plane wave exposure. In particular, different tendency was observed between the ambient heat and RF exposures. When the pregnant woman model was exposed to ambient temperature of 35–45 °C, the core temperature elevations in the mother and the foetus are almost identical. On the contrary, the foetal temperature elevation for RF exposure is higher than

that in the mother. This higher temperature elevation in the foetus becomes obvious, particularly when relative large electromagnetic energy absorption occurs in and around the foetus.

ACKNOWLEDGEMENTS

This research was supported in part by Strategic International Cooperative Program (Joint Research Type), Japan Science and Technology Agency and the France National Research Agency.

REFERENCES

1. V. De Santis and M. Feliziani, "Effects of thermoregulatory mechanisms on the eye thermal elevation produced by intense RF exposures," *Proc. IEEE Int'l Symp Electromagnetic Compatibility*, pp.1-6, 2008.
2. M. Kilic and G. Sevilgen, "Evaluation of heat transfer characteristics in an automobile cabin with a virtual manikin during heating period," *Numerical Heat Transfer, Part A: Applications,* vol. 56, pp. 515-539, 2009.
3. X. Zeng, W. Dai, and A. Bejan, "Vascular countercurrent network for 3-D triple-layered skin structure with radiation heating," *Numerical Heat Transfer, Part A: Applications,* vol. 57, pp. 369-391, 2010.
4. A. Sakurai, S. Maruyama, K. Matsubara, "The radiation element method coupled with the bioheat transfer equation applied to the analysis of the photothermal effect of tissues," *Numerical Heat Transfer, Part A: Applications,* vol. 58, pp. 625-640, 2010.
5. A. Ghazy and D. J. Bergstrom, "Numerical simulation of transient heat transfer in a protective clothing system during a flash fire exposure," *Numerical Heat Transfer, Part A: Applications,* vol. 58, pp. 702-724, 2010.
6. K. -C. Liu, C. -T. Lin, "Solution of an inverse heat conduction problem in a bi-layered spherical tissue," *Numerical Heat Transfer, Part A: Applications,* vol. 58, pp. 802-818, 2010.
7. N. Afrin, J. Zhou, Y. Zhang, D. Y. Tzou, J. K. Chen, "Numerical simulation of thermal damage to living biological tissues induced by laser irradiation based on a generalized dual phase lag model," *Numerical Heat Transfer, Part A: Applications,* vol. 61, pp. 483-501, 2012.
8. M. A. S. Harvey, M. M. McRorie, and D. W. Smith, "Suggested limits to the use of the hot tub and sauna by pregnant women," *Canadian Medical Association Journal,* vol. 125, p. 50, 1981.
9. WHO. (2006, Feb. 21). *Research Agenda for Radio Frequency Fields http://www.who.int/peh-emf/research/rf_research_agenda_2006.pdf.*
10. IEC, Medical electrical equipment: part 2-33. Particular requirements for basic safety and essential performance of magnetic resonance equipment for medical diagnosis IEC 60601-2-33, 2002.

11. D. Wu, S. Shamsi, J. Chen and W. Kainz, "Evaluations of specific absorption rate and temperature increase within pregnant female models in magnetic resonance imaging birdcage coils, " *IEEE Trans. Microwave Theory & Tech,* vol. 54, pp. 4472-4478, 2006.
12. J. Hand, Y. Li, and J. Hajnal, "Numerical study of RF exposure and the resulting temperature rise in the foetus during a magnetic resonance procedure," *Phys. Med. Biol.,* vol. 55, p. 913, 2010.
13. ICNIRP, "Guidelines for limiting exposure to time-varying electric, magnetic, and electromagnetic fields (up to 300 GHz)," *Health Phys.,* vol. 74, pp. 494-521, 1998.
14. I. Laakso and A. Hirata, "Dominant factors affecting temperature rise in simulations of human thermoregulation during RF exposure," *Phys. Med. Biol.,* vol. 56, p. 7449, 2011.
15. S. Kikuchi, K. Saito, M. Takahashi, and K. Ito, "Temperature elevation in the fetus from electromagnetic exposure during magnetic resonance imaging," *Phys. Med. Biol.,* vol. 55, p. 2411, 2010.
16. A. Hirata, T. Asano, and O. Fujiwara, "FDTD analysis of human body-core temperature elevation due to RF far-field energy prescribed in the ICNIRP guidelines," *Phys. Med. Biol.,* vol. 52, pp. 5013-5023, 2007.
17. P. Gowland and J. De Wilde, "Temperature increase in the fetus due to radio frequency exposure during magnetic resonance scanning," *Physics in Medicine and Biology,* vol. 53, pp. L15-L18, 2008.
18. H. Asakura, "Fetal and neonatal thermoregulation," *J. Nippon Med. School,* vol. 71, pp. 360-370, 2004.
19. T. Nagaoka, S. Watanabe, K. Sakurai, E. Kunieda, M. Taki, and Y. Yamanaka, "Development of realistic high-resolution whole-body voxel models of Japanese adult males and females of average height and weight, and application of models to radio-frequency electromagnetic-field dosimetry," *Phys. Med. Biol.,* vol. 49, pp. 1-15, 2004.
20. T. Yamanishi, T. Kamai, and K. I. Yoshida, "Neuromodulation for the treatment of urinary incontinence," *Int'l J Urology,* vol. 15, pp. 665-672, 2008.
21. H. H. Pennes, "Analysis of tissue and arterial blood temperatures in the resting human forearm," *J. Appl. Physiol.,* vol. 1, pp. 93-122, 1948.
22. A. Hirata and O. Fujiwara, "Modeling time variation of blood temperature in a bioheat equation and its application to temperature analysis due to RF exposure," *Phys. Med. Biol.,* vol. 54, pp. N189-N196, 2009.
23. A. Hirata, I. Laakso, T. Oizumi, R. Hanatani, K. H. Chan, and J. Wiart, "The relationship between specific absorption rate and temperature elevation in anatomically based human body models for plane wave exposure from 30 MHz to 6 GHz," *Phys. Med. Biol.,* vol. 58, p. 903, 2013.

24. D. Fiala, K. J. Lomas, and M. Stohrer, "A computer model of human thermoregulation for a wide range of environmental conditions: The passive system," *J. Appl. Physiol.,* vol. 87, pp. 1957-1972, 1999.
25. D. Fiala, K. J. Lomas, and M. Stohrer, "Computer prediction of human thermoregulatory and temperature responses to a wide range of environmental conditions," *Int. J. Biometeorology,* vol. 45, pp. 143-159, 2001.
26. A. Hirata, T. Asano, and O. Fujiwara, "FDTD analysis of body-core temperature elevation in children and adults for whole-body exposure," *Phys. Med. Biol.,* vol. 53, pp. 5223-5238, 2008.
27. F. A. Duck, *Physical properties of tissue: a comprehensive reference book*: Academic Pr, 1990.
28. M. Fall, C.-A. Carlsson, and B.-E. Erlandson, "Electrical stimulation in interstitial cystitis," *J. Urology,* vol. 123, p. 192, 1980.
29. P. Bernardi, M. Cavagnaro, S. Pisa, and E. Piuzzi, "Specific absorption rate and temperature elevation in a subject exposed in the far-field of radio-frequency sources operating in the 10-900-MHz range," *IEEE Trans. Biomed. Eng.,* vol. 50, pp. 295-304, 2003.
30. J. A. J. Stolwijk, "Mathematical model of physiological temperature regulation in man," *NASA Contractor Reports,* 1971.
31. P. J. Dimbylow, A. Hirata, and T. Nagaoka, "Intercomparison of whole-body averaged SAR in European and Japanese voxel phantoms," *Phys. Med. Biol.,* vol. 53, pp. 5883-5897, 2008.
32. S. Gabriel, R. W. Lau, and C. Gabriel, "The dielectric properties of biological tissues: III. Parametric models for the dielectric spectrum of tissues," *Phys. Med. Biol.,* vol. 41, p. 2271, 1996.
33. P. J. Dimbylow, "FDTD calculations of the whole-body averaged SAR in an anatomically realistic voxel model of the human body from 1 MHz to 1 GHz," *Phys. Med. Biol.,* vol. 42, pp. 479-490, 1997.
34. A. Hirata, M. Fujimoto, T. Asano, J. Wang, O. Fujiwara, and T. Shiozawa, "Correlation between maximum temperature increase and peak SAR with different average schemes and masses," *IEEE Trans. Electromagnet. Compat.,* vol. 48, pp. 569-577, 2006.
35. T. Samaras, E. Kalampaliki, and J. N. Sahalos, "Influence of Thermophysiological Parameters on the Calculations of Temperature Rise in the Head of Mobile Phone Users," *IEEE Trans. Electromagnet. Compat.,* vol. 49, pp. 936-939, 2007.
36. M. Murbach, E. Neufeld, W. Kainz, K. P. Pruessmann, and N. Kuster, "Whole-body and local RF absorption in human models as a function of anatomy and position within 1.5 T MR body coil," *Mag. Reson. Med.,* 2013.

Figure Captions

Figure 1. Numerical pregnant woman model and its temperature distribution at the thermally steady state without heat load. Elliptic dots approximately represent the position of amniotic fluid.

Figure 2. Blood temperature variations in the foetus and its mother for different ambient temperatures (35, 40, and 45 °C).

Figure 3. Blood temperature variations in the foetus and its mother for whole-body averaged SAR of 2 and 4 W/kg for plane wave exposure at a frequency of 80 MHz.

Figure 4. (a) Blood temperature of the foetus and its mother for different whole-body averaged SARs and frequencies and (b) its relative difference.

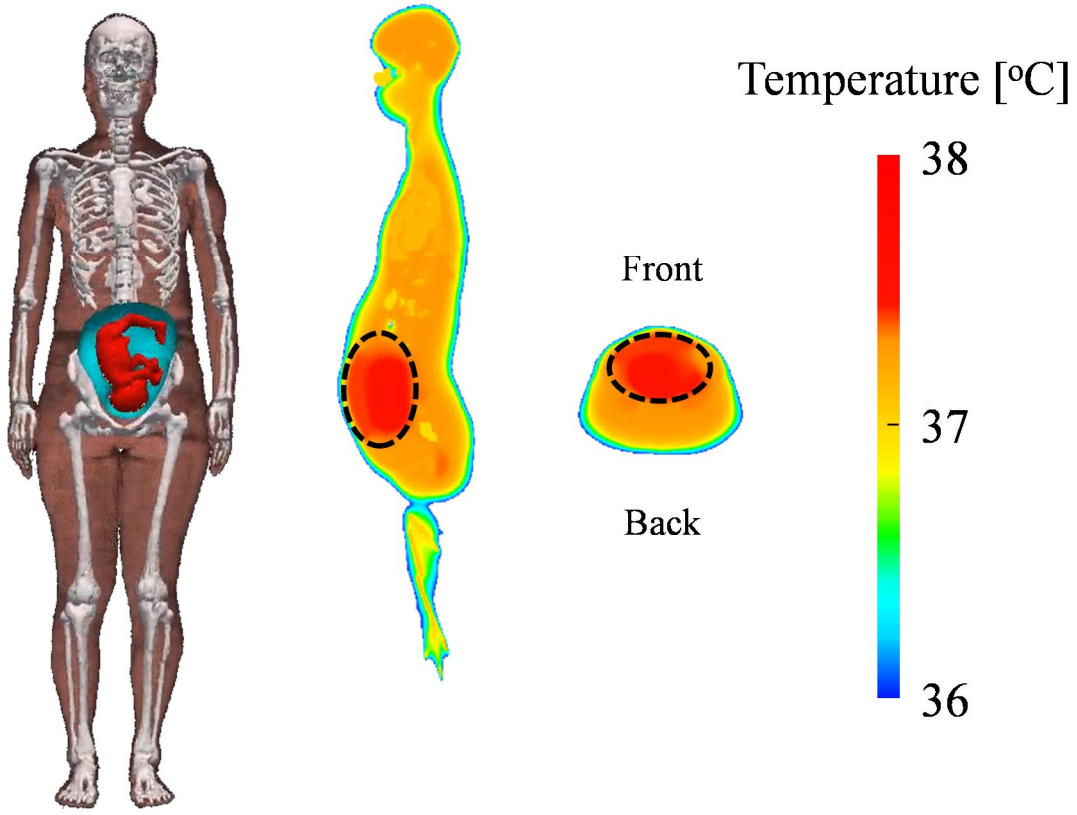

Fig. 1.

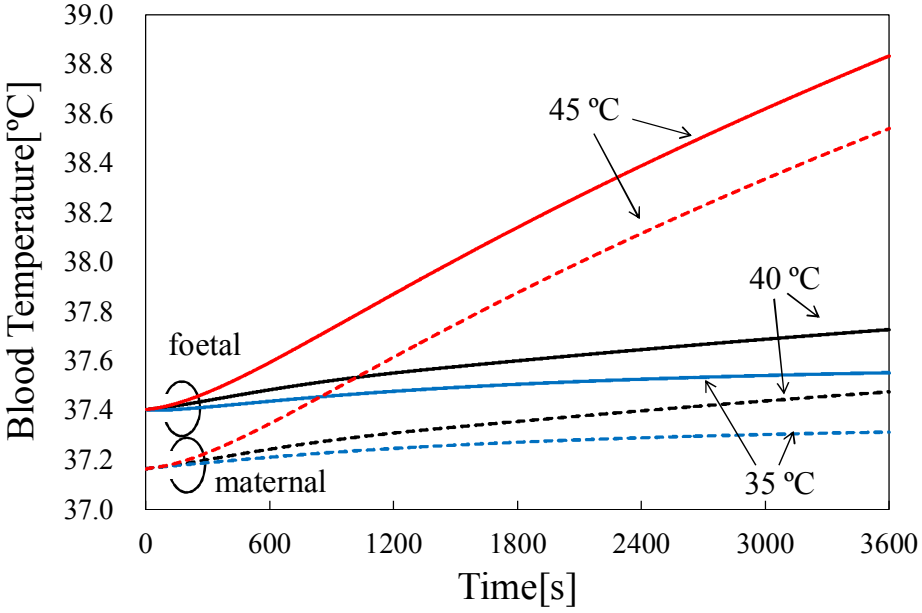
Blood Temperature[ºC]
39.0
38.8
38.6
38.4
38.2
38.0
37.8
37.6
37.4
37.2
37.0
45 ºC
40 ºC
35 ºC
foetal
maternal
0
600
1200
1800
2400
3000
3600
Time[s]

Fig. 2.

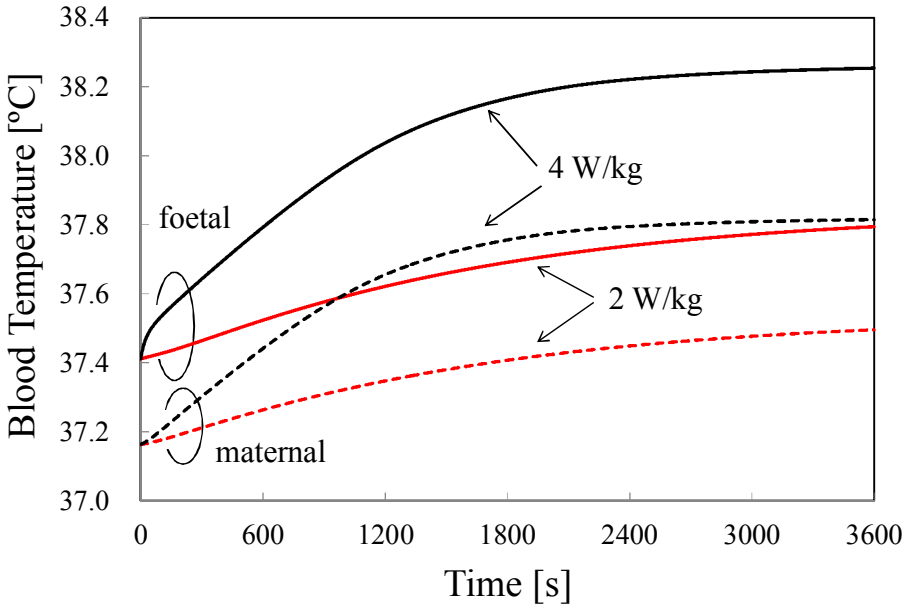
38.4
38.2
38.0
37.8
37.6
37.4
37.2
37.0
Blood Temperature [°C]
foetal
maternal
4 W/kg
2 W/kg
0
600
1200
1800
2400
3000
3600
Time [s]

Fig. 3.

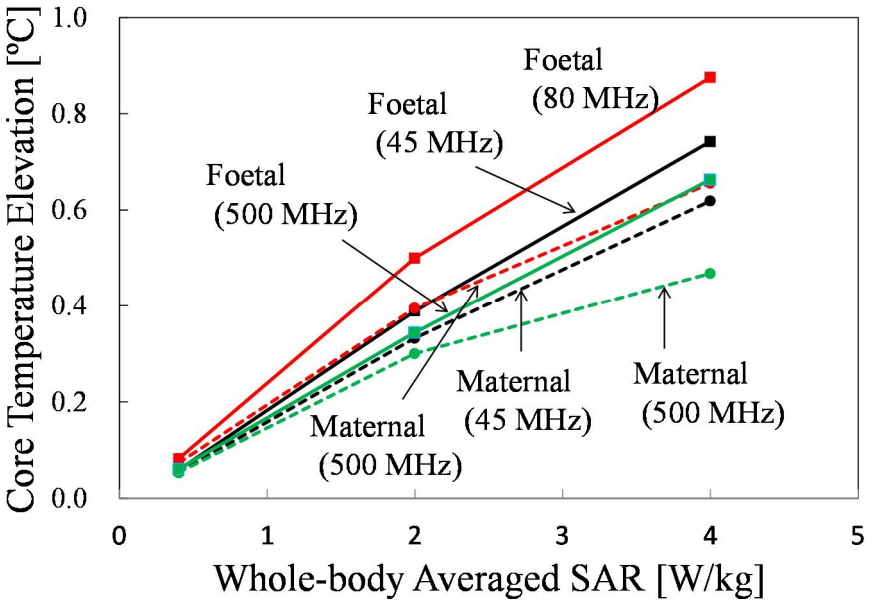
Core Temperature Elevation [°C]
1.0
0.8
0.6
0.4
0.2
0.0
0
1
2
3
4
5
Whole-body Averaged SAR [W/kg]
Foetal (80 MHz)
Foetal (45 MHz)
Foetal (500 MHz)
Maternal (45 MHz)
Maternal (500 MHz)
Maternal (500 MHz)

(a)

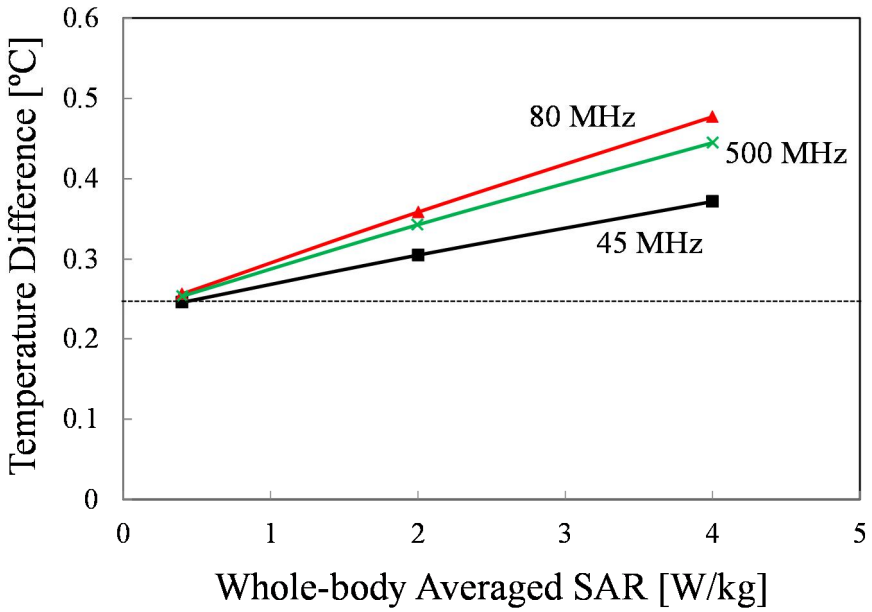
Temperature Difference [°C]
0.6
0.5
0.4
0.3
0.2
0.1
0
0
1
2
3
4
5
Whole-body Averaged SAR [W/kg]
80 MHz
500 MHz
45 MHz

(b)

Fig. 4.